Songklanakarin J. Sci. Technol.
42 (2), 415-423, Mar. - Apr. 2020

http://www.sjst.psu.ac.th

Original Article

Computational study on two-phase MHD buoyancy driven flow in an asymmetric diverging channel

Sadhu Ramprasad[1*], S. H. C. V. Subba Bhatta[1], and Bandaru Mallikarjuna[2]

[1] *Department of Mathematics, M. S. Ramaiah Institute of Technology, Bangalore, Karnataka, 560054 India*

[2] *Department of Mathematics, B. M. S. College of Engineering, Bangalore, Karnataka, 560019 India*

Received: 8 July 2018; Revised: 9 January 2019; Accepted: 20 January 2019

Abstract

In this paper the problem of a two-dimensional steady viscous, incompressible two-phase flow of a particulate suspension in an asymmetric diverging channel with a heat source is considered. The differential equations governing the flow are non-dimentionalized by employing suitable transformations and resulting equations are solved numerically, using Runge-Kutta Shooting technique. The influence of Magnetic parameter, Reynolds number, Cross flow Reynolds number, Grash of number, heat source parameter, Prandtl number are exhibited graphically and velocity and temperature profiles for both fluid as well as particle phases discussed. Computational values for skin friction coefficient, Nusselt number are obtained and presented in tabular form and discussed. This study plays an important role in many engineering and biological fields such as cooling of nuclear reactors, chemical and food industries, blood flow through capillaries and arteries.

Keywords: MHD, particulate suspension, two-phase flow, diverging channel

1. Introduction

Study of flow through spatially varying geometries like converging or diverging channels is of great importance in aerospace, industrial, environmental and biomechanical engineering as well as in understanding flow over rivers and canals. An incompressible viscous fluid flow between two non-parallel plates was first studied by Jeffery (1915). Banks, Drazin, and Zaturska (1988) used analytical method to study Jeffrey-Hamel flow. Terril (1965) investigated by taking into account transpiration effects and presented analytical solutions for slow flow through a non-uniform channel. An extensive amount of study has been performed in the last few decades on convergent and divergent channels by Gerdroodbary, Rahimi, and Ganji (2015), Ghaedamini, Lee, and Teo (2013), Mustafa (2014), Rita and Kamal (2011) etc. Sinharoy and Nayak (1982) investigated steady two-dimensional laminar viscoelastic fluid flow in a non-uniform channel. Homotopy perturbation method (HPM) is used to find an analytical solution for Magnetohydrodynamics (MHD) flow of viscoelastic fluids in non-uniform channels by Shadloo and Kimiaeifar (2010). Verma, Aruna, and Jeevan (1998) studied steady two dimensional magnetic fluid flow in a diverging channel in the presence of an external magnetic field. Sahoo and Sastri (1997) investigated numerically natural convective flow of viscous fluid in a divergent channel. Yilmaz, Akyatan, and Senocak (1998) discussed two dimensional flow of the Reiner-Rivlin fluid in non-uniform porous channels**.**

Study of electrically conducting fluid flowing through channels is useful in industrial and biological systems such as MHD accelerator technologies and hydro-magnetic energy generators. Alam and Khan (2014) used finite element method to investigate MHD effects on mixed convective flow through a diverging channel with circular obstacle. Mir, Umar, Naveed, Raheela, and Syed (2013) investigated MHD flow of a Jeffery fluid in converging and diverging channels. Hatami, Sheikholeslami, Hosseini, and Ganji (2014) studied

*Corresponding author
Email address: sadhurp@gmail.com

analytically MHD nanofluid flow in a non parallel channel. Nano fluid flow and heat transfer in an asymmetric porous channel with expanding and contracting wall was studied numerically by Hatami, Sheikholeslami, and Ganji (2014), Mallikarjuna, Rashad, Chamkha, and Hariprasad (2016) investigated MHD flow of an incompressible viscous fluid from a rotating vertical cone in porosity regime. Mohammadreza and Rouzbeh (2016) investigated MHD copper-water nanofluid flow and heat transfer through a convergent-divergent channel. Umarkhan, Naveed, and Syed (2015) presented heat and mass transfer analysis for viscous incompressible fluid in converging and diverging channel and studied Soret and Dufour effects. Fakour, Vahabzadeh, Ganji, and Hatami (2015) investigated analytically heat transfer of a micropolar fluid in a channel with penetrable walls. Ghadikolaei, Hosseinzadeh, Yassari, Sadeghi, and Ganji (2018) studied second grade fluid flow on a streching sheet analytically and compared the result with numerical solution.

Two-phase flow of particulate suspension applications abound in many areas of technology: food industries, powder technology, waste water treatment, combustion and corrosive particles in engine oil flow etc. So it is important to study fluid-particle hydromagnetic convective flows in order to understand the influence of the different phases on heat transfer processes. Recently, a remarkable number of researchers, Sivakumar, Sreenath, and Pushpavanam **(**2010**)**, Hatami, Hosseinzadeh, Domairry, and Behnamfar (2014) have investigated two-phase particulate flows with and without magnetic field and heat transfer analytically and numerically. Chamkha (1995) studied hydromagnetic two-phase flow in a channel. Mansour and Chamkha (2003) developed a continuum model to analyze heat generation effects on two-phase particulate suspension MHD flow through a channel. Usha, Senthilkumar, and Tulapurkara (2006) investigated particulate suspension flow in a travelling wavy channel. Heat generation effects on hydromagnetic flow of a particulate suspension through isothermal-isoflux channels was investigated by Chamkha and Rashidi (2010). Rawat *et al*. (2014) presented a numerical model for steady two dimensional two-phase hydromagnetic flows and heat transfer in a particulate-suspension through a non-Darcian porous channel. Sadia, Naheed, and Anwar (2017) studied compressible dusty gas along a vertical wavy surface. Krupalakshmi, Gireesha, Gorla, and Mahanthesh (2016) investigated numerically laminar boundary layer flowheat and mass transfer of two-phase particulate suspension past a stretching sheet with chemical reaction. Mohammad, Islam, Prilal, Ramzan, and Abumandown (2015**)** investigated peristaltic transport of a particle-fluid suspension in a planar channel by taking slip effects on the wall into account. Eldesoky, Abdelsalam, Abumandown, Kamel, and Vafai (2017) analytically studied interaction between compressibility and particulate suspension on peristaltically driven flow in a planar channel. Mallikarjuna, Rashad, Hussein, and Hariprasad (2016) studied numerically the effects of transpiration, thermal radiation and thermophoresis effects on convective flow over a rotating cone in a non-Darcy porous medium. Recently Ramprasad, Subba Bhatta, and Mallikarjuna (2018) considered velocity and temperature slip effects and studied numerically particulate suspension flow in a divergent channel.

With the available literature and to the best of the authors knowledge, no one has studied convective two-phase flow in an asymmetric divergent channel. Keeping in view the above facts, a mathematical model has been developed to study MHD convective two-phase particulate suspension flow in a divergent channel with heat source.

2. Model of the Problem

Consider steady, viscous, two-dimensional incompressible laminar two-phase flow of particulate suspension in an asymmetric diverging channel. Walls of the channel are placed at $\theta = \pm\alpha$ as shown in Figure 1. Suction/injection velocities are assumed at different walls and these velocities are to be varied inversely proportional to the distance along the wall from origin of the channel. The continuity equation, the Navier–Stokes equations and the energy equation governing the flow in polar coordinates (r,θ) are given by Terril (1965) and Baris (2003)

For fluid phase

$$\frac{\partial}{\partial r}(ru)+\frac{\partial v}{\partial \theta}=0, \tag{1}$$

$$\left(u\frac{\partial u}{\partial r}+\frac{v}{r}\frac{\partial u}{\partial \theta}-\frac{v^2}{r}\right)=-\frac{1}{\rho}\frac{\partial p}{\partial r}+\upsilon\left[\left(\frac{\partial^2 u}{\partial r^2}+\frac{1}{r}\frac{\partial u}{\partial r}+\frac{1}{r^2}\frac{\partial^2 u}{\partial \theta^2}\right)-\frac{u}{r^2}+\frac{2}{r^2}\frac{\partial v}{\partial \theta}\right]+\frac{\rho_p}{\rho}S\left(u_p-u\right)-\frac{\sigma H_0^{\,2}\mu_e^{\,2}u}{\rho}-g\beta^* T, \tag{2}$$

$$\left(u\frac{\partial v}{\partial r}+\frac{v}{r}\frac{\partial v}{\partial \theta}+\frac{uv}{r}\right)=-\frac{1}{\rho r}\frac{\partial p}{\partial \theta}+\upsilon\left[\left(\frac{\partial^2 v}{\partial r^2}+\frac{1}{r}\frac{\partial v}{\partial r}+\frac{1}{r^2}\frac{\partial^2 v}{\partial \theta^2}\right)-\frac{v}{r^2}+\frac{2}{r^2}\frac{\partial u}{\partial \theta}\right]+\frac{\rho_p}{\rho}S\left(v_p-v\right), \tag{3}$$

$$u\frac{\partial T}{\partial r}+\frac{v}{r}\frac{\partial T}{\partial \theta}=\frac{k}{\rho c_p}\left(\frac{1}{r}\frac{\partial}{\partial r}\left(r\frac{\partial T}{\partial r}\right)+\frac{1}{r^2}\frac{\partial^2 T}{\partial \theta^2}\right)+\frac{Q_0}{\rho c_p}T+\frac{\rho_p C_m}{\tau_T \rho c_p}\left(T_p-T\right), \tag{4}$$

For particle phase

$$\frac{\partial}{\partial r}\left(ru_p\right)+\frac{\partial v_p}{\partial \theta}=0, \tag{5}$$

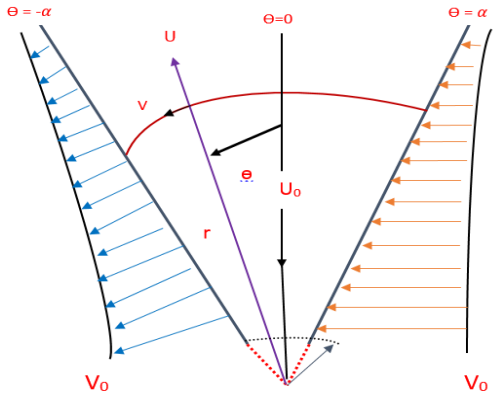

Figure 1. Geometry of the flow

$$\left(u_p\frac{\partial u_p}{\partial r}+\frac{v_p}{r}\frac{\partial u_p}{\partial \theta}-\frac{v_p^{\,2}}{r}\right)=-\frac{1}{\rho_p}\frac{\partial p}{\partial r}+S\left(u-u_p\right)-g\beta^{*}T_p, \tag{6}$$

$$\left(u_p\frac{\partial v_p}{\partial r}+\frac{v_p}{r}\frac{\partial v_p}{\partial \theta}+\frac{u_p v_p}{r}\right)=-\frac{1}{r\rho_p}\frac{\partial p}{\partial \theta}+S\left(v-v_p\right), \tag{7}$$

$$u_p\frac{\partial T_p}{\partial r}+\frac{v_p}{r}\frac{\partial T_p}{\partial \theta}=\frac{1}{\tau_T}\left(T-T_p\right), \tag{8}$$

The associated boundary conditions are

$$\begin{aligned}&u=0,u_p=0\ \ at\,\theta=\pm\alpha\quad u\left(\theta=0\right)=U_0\\&T=T_w,T_p=T_{w_p}\ at\ \theta=\pm\alpha\end{aligned} \tag{9}$$

Introducing the following dimensionless variables

$$u=\frac{U_0 r_0 f(\theta)}{r};u_p=\frac{U_0 r_0 g(\theta)}{r};v_p=\frac{V_{p_0} r_0}{r};v=\frac{V_0 r_0}{r};\ h=\frac{T}{T_w};\ H=\frac{T}{T_{w_p}}$$

4. Solution Methodology

A set of equations (10) – (13) with boundary con-ditions (14) are first rewritten in a system of first order equations by assuming $f=f(1),\ f'=f(2),\ f''=f(3),\ g=f(4),g'=f(5),h=f(6),\ \ h'=f(7),H=f(8),\ \ H'=f(9)$, i.e.

$$\frac{dY}{dx}=\frac{d}{dx}\begin{bmatrix}f(1)\\f(2)\\f(3)\\f(4)\\f(5)\\f(6)\\f(7)\\f(8)\\f(9)\end{bmatrix}=\begin{bmatrix}f(2)\\f(3)\\f'''=-2\mathrm{Re}\,f(1)f(2)+Rf(3)-L\beta\left(f(5)-f(2)\right)-\left(4-M^2\right)f(2)+\dfrac{Gr}{\mathrm{Re}}f(7)\\f(5)\\g''=2\dfrac{\mathrm{Re}}{R}f(4)f(5)+\dfrac{\beta}{R}\left(f(2)-f(5)\right)+\dfrac{Gr}{\mathrm{Re}\,R}f(9)\\f(7)\\h''=R\,\mathrm{Pr}\,f(7)-\mathrm{Pr}\,Qf(6)-L\beta_t\,\mathrm{Pr}\,\gamma\left(f(8)-f(6)\right)\\f(9)\\H''=K\left(f(7)-f(9)\right)\end{bmatrix} \tag{15}$$

We choose some initial conditions $f'(-\alpha)=c_1,\ f''(-\alpha)=c_2,g'(-\alpha)=c_3,\ \ h'(-\alpha)=c_4,$ and $H'(-\alpha)=c_5$ which are not given at initial point and integrate (15) using Runge-Kutta fourth order technique (Ghadikolaei, Hosseinzadeh, & Ganji, 2018;

Equation (1) – (9) are reduced to

$$f'''+2\mathrm{Re}\,ff''-Rf''+L\beta\left(g'-f'\right)+\left(4-M^2\right)f'-\frac{Gr}{\mathrm{Re}}h'=0, \tag{10}$$

$$g''-2\frac{\mathrm{Re}}{R}gg'-\frac{\beta}{R}\left(f'-g'\right)-\frac{Gr}{\mathrm{Re}\,R}H'=0, \tag{11}$$

$$h''-R\,Prh'+PrQh+L\beta_t\gamma Pr\left(H-h\right)=0, \tag{12}$$

$$H'-K\left(h-H\right)=0\,, \tag{13}$$

Associated boundary conditions are

$$\begin{aligned}&f\left(\pm\alpha\right)=0,\ f\left(0\right)=1\\&g\left(\pm\alpha\right)=0,h\left(\pm\alpha\right)=1,H\left(\pm\alpha\right)=1\end{aligned} \tag{14}$$

3. Skin Friction Coefficient and Nusselt Number

The main aim of the physical interest of the problem is analyzing drag coefficient and rate of heat transfer over surface of the channel, which are defined by skin friction

$$C_f=\frac{\tau_s}{\rho U_o^2}=\frac{\mu\left(\dfrac{\partial u}{r\partial\theta}\right)_{\theta=\pm\alpha}}{\rho U_o^2}$$ and Nusselt number

$$Nu=\frac{rq_s}{\kappa T_w}=\frac{r\left(\dfrac{-\kappa\partial T}{r\partial\theta}\right)_{\theta=\pm\alpha}}{\kappa T_w}$$

In non-dimensional form

$$C_f=\frac{1}{\mathrm{Re}}f'\left(\pm\alpha\right)\text{ and }Nu=-h'\left(\pm\alpha\right)$$

Gholinia, Gholinia, Hosseinzadeh, & Ganji, 2018; Mallikarjuna, Rashad, Chamkha, & Hariprasad Raju, 2016; Mallikarjuna, Rashad, Hussein, & Hariprasad Raju, 2016). The obtained results were compared at α and differences attributed wrong assumptions of the initial conditions. To overcome the problem, we applied Newton Raphson method to choose the initial conditions and integrated Equation (15) using RK4 with a step size of 0.001 with 10^{-4} accuracy for the solutions. To validate the present code, the results are compared in the absence of energy equation, thermal buoyancy and heat source with existing results produced by Ramprasad, Subba Bhatta, Mallikarjuna, and Srinivasacharya (2017). The obtained results were found to be good agreement as shown in Table 1. In this section we studied the role of non-dimensional flow parameters embedded in the flow model on fluid and particle phase velocities and temperatures.

5. Results and Discussion

For numerical calculations we fixed the non-dimensional parameter values as R=1, Re=0.5, M=1.5, Gr=5, L=1, Pr=0.71, Q=0.5, $\alpha = \frac{\pi}{4}$, $\gamma = 0.5, \beta = 1$ $\beta_t = 0.5$. These values were maintained constant in the whole study excluding dissimilarities in the particular figures.

Figures 2-4 depict the profiles of fluid velocity with variations in different governing parameters M, R, and Gr. As M, the Lorentz force which opposes the flow, increases the velocity of the fluid phase decreases as shown in Figure 2. This is in good agreement with Chamkha and Rashidi (2010), and Mir Asadullah, Umar, Naveed, Raheela, and Syed (2013). It can be concluded that the flow can be controlled by imposing higher magnetic field on the boundaries. Figure 3 illustrates that with an increase in R the velocity of the fluid decreases in the left half of the channel whereas it increases in right half of the channel enormously. Near the wall $\alpha = \frac{\pi}{4}$ the viscosity effects are very small therefore the velocity attains maximum near that wall. This is in good agreement with Roy and Nayak (1982), and Terril (1965). Figure 4 always that an increase in Gr leads to increase in gravitational force and dominates the thermal buoyancy force. It causes a decrease in the fluid velocity throughout the channel.

Figures 5 to 7 represent the variation of particle phase velocity with different variations in governing parameters M, R, and Gr. From Figure 5 it is evident that with a hike in M, an enhancement of the particle phase velocity is observed in the left part of channel and opposite behavior is observed in right part of the channel. This is in good agreement with Mansour and Chamkha (2003). From Figure 6 it is observed that with an increase in R the particle phase velocity increases in the left half of the channel and the reverse behavior is observed in the right half of the channel. Figure 7 shows that with an increase in Gr, the thermal buoyancy effect increases. This gives rise to accelerated particle phase velocity in the entire channel. The same observation has been reported by Chamkha and Rashidi (2010).

The influence of Prandtl number Pr, on fluid temperature is depicted in Figure 8. It can be seen from this figure that the temperature of fluid increases rapidly with an increment in Pr. This indicates that momentum diffusivity dominates over the fluid temperature. If Pr=0.6 the fluid is oxygen and if Pr=0.71 it is air. If Pr = 1.3 the fluid is gaseous ammonia. Figure 9 anticipates the behavior of heat source parameter Q on fluid phase temperature. As Q increases the fluid phase temperature increases and maximum temperature is attained in the mid region of the channel. Figure 10 explains the behavior of R on fluid tempearture. As R increases the fluid temperature gradually decreases in the entire channel. From Figure 11 it is observed that with an increase in Pr the temperature of the particle phase increases over the left part of channel and decreases in the right part of the channel. This means that momentum diffusivity in greater in the right part of the channel and lower in the left part of the channel. An increment in Q enhances the particle temperature in the left side of the channel and opposite trend is observed in the right part of the channel as demonstrated in Figure 12. Figure 13 demonstrates that with an increase in R the particle phase temperature decreases in the left half of the channel and increases in the right half of the channel.

From Table 2 it is observed that with an increase in R, the skin friction coefficient (C_f) decreases and the Nusselt number (Nu) is enhanced near both the walls. As Re increases the skin friction coefficient decreases on left wall and increases on right wall with no change in Nusselt number over both walls. As β increases C_f decreases near both the walls, but Nu remains constant at both the walls. This indicates that interaction of fluid and particles does not influence the rate of heat transfer over the walls. As β_t skin friction coefficient increases on the left wall and decreases on right, the Nusselt number decreases at both the walls.

Table 1. Comparison results of skin friction coefficient for M = 0, Gr = 0, Pr = 0, Q = 0, $\gamma = 0$, $\beta = 1$

R	Re	β	α	L	Present results		Ramprasad, Subba Bhatta , Mallikarjuna, and Srinivasacharya (2017)	
					$f'(-\alpha)$	$f'(\alpha)$	$f'(-\alpha)$	$f'(\alpha)$
1	1	1	$\pi/6$	0.5	2.781459	-4.221980	2.780681	-4.235391
3					2.056121	-6.54466	2.060452	-6.55393
5					1.770238	-9.684489	1.774729	-9.691618
8					1.689143	-15.381343	1.692932	-15.385567
1	3				2.545961	-4.049399	2.544912	-4.063783
	5				2.304533	-3.884566	2.303143	-3.900072

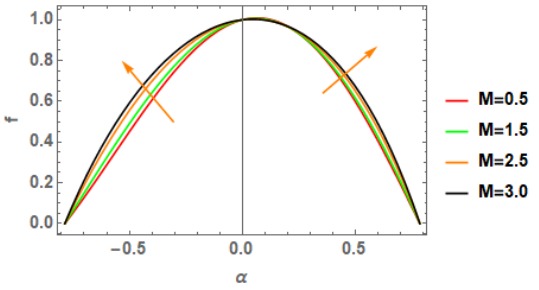

Figure 2. Effect of M on fluid phase velocity

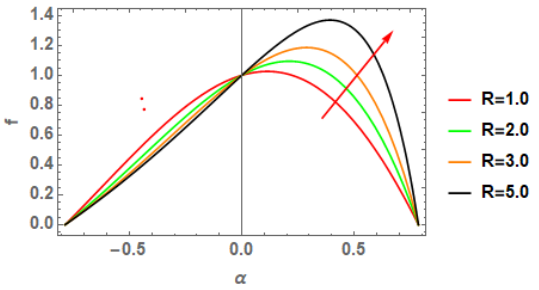

Figure 3. Effect of R on fluid phase velocity

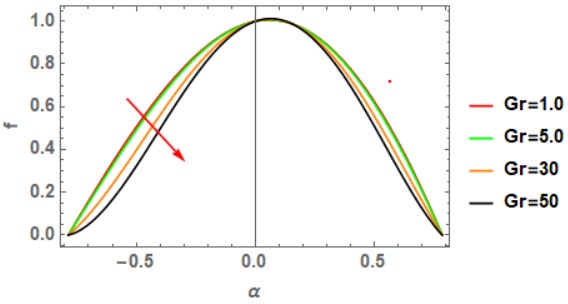

Figure 4. Effect of Gr on fluid phase velocity

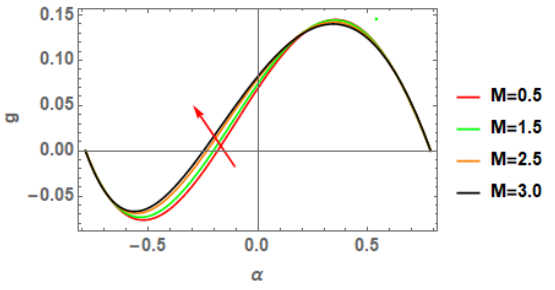

Figure 5. Effect of M on particle phase velocity

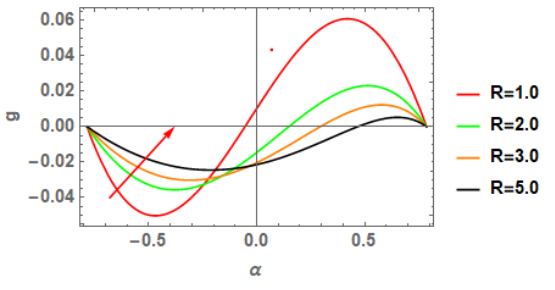

Figure 6. Effect of R on particle phase velocity;

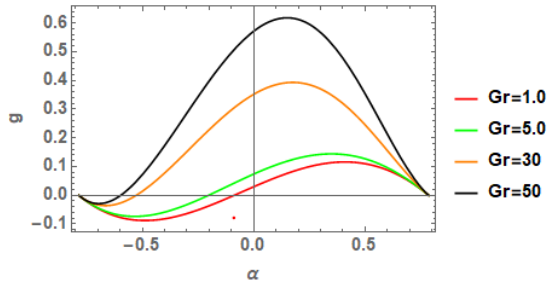

Figure 7. Effect of Gr on particle phase velocity

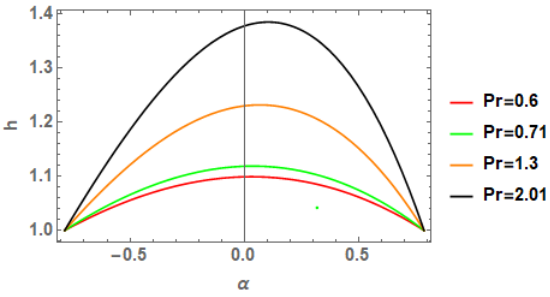

Figure 8. Effect of Pr on fluid phase temperature

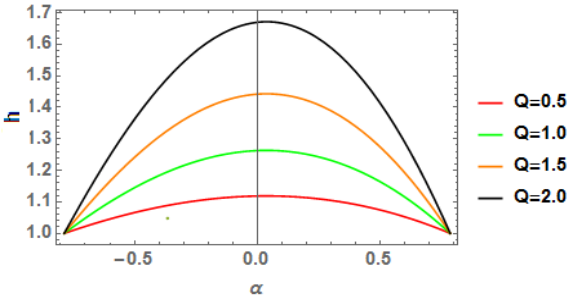

Figure 9. Effect of Q on fluid phase temperature

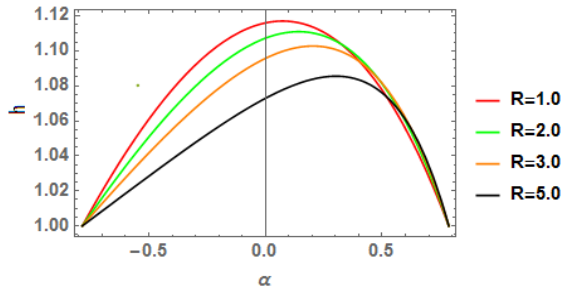

Figure 10. Effect of R on fluid phase temperature

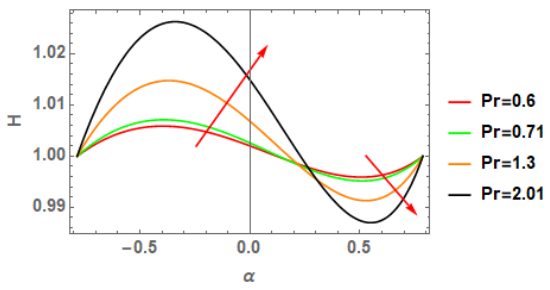

Figure 11. Effect of Pr on particle phase temperature

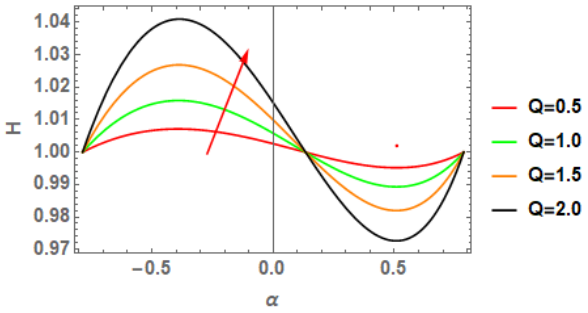

Figure 12. Effect of Q on particle phase temperature

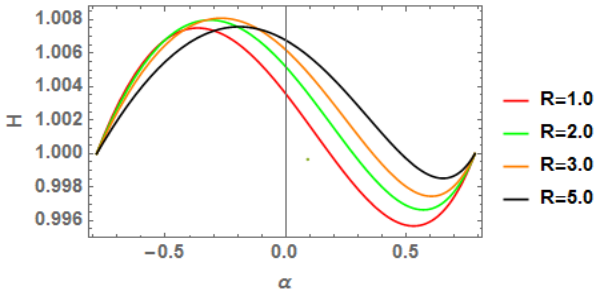

Figure 13. Effect of R on particle phase temperature

Table 2. Skin friction and Nusselt number values for different values of R, Re, β and β_t.

R	Re	β	β_t	$f'(-\alpha)$	$f'(\alpha)$	$-h'(-\alpha)$	$-h'(\alpha)$
0.5	0.5	0.5	0.5	1.0096228	-1.994494	-0.270335	0.326925
1				0.723166	-2.698527	-0.242619	0.354009
3				0.412281	-6.762408	-0.152345	0.438818
5				0.395312	-11.741687	-0.100142	0.484577
0.5	1			0.995183	-2.010839	-0.270335	0.326925
0.5	2			0.823061	-1.9459951	-0.270335	0.326925
0.5	3			0.604042	-1.882062	-0.270335	0.326925
	0.5	1		1.014167	-2.0156504	-0.270335	0.326925
		2		1.004385	-2.054682	-0.270335	0.326925
		3		0.986932	-2.07792	-0.270335	0.326925
		5		0.960786	-2.093595	-0.270335	0.326925
		0.5	1	1.0102835	-1.995061	-0.268621	0.324332
			2	1.0108763	-1.996580	-0.266159	0.319972
			3	1.010932	-1.998231	-0.264778	0.316865

From Table 3 it is noted that as γ increases the skin friction coefficient increases on the left wall and decreases on the right wall. The same behavior is observed in the Nusselt number. With an increase in L skin friction coefficient on left wall and a decrease on the right wall, the same results are observed on the Nusselt number. An increment in Q reduces the skin friction coefficient and Nusselt number at the left wall whereas the reverse behavior is observed at the right wall. As M increases skin friction coefficient decreases on both walls. Nusselt number values do not change at either wall with increasing values of M.

6. Conclusions

In this paper, the flow of a viscous incompressible fluid through a divergent channel in a particulate suspension with MHD and heat generation has been discussed. Numerical method has been applied to solve non-linear differential equations by non-dimensionalising using suitable transformations. The conclusions of present study are as follows.

1) With an increase in Gr, the fluid velocity decreases whereas the particle phase velocity increases.

Table 3. Skin friction and Nusselt number values for different values of γ, L, Q and M

γ	L	Q	M	$f'(-\alpha)$	$f'(\alpha)$	$-\theta'(-\alpha)$	$-\theta'(\alpha)$
1	0.2	0.5	1.5	1.011476	-1.995832	-0.268373	0.324245
2				1.015080	-1.998435	-0.264552	0.319032
3				1.018553	-2.000947	-0.260863	0.314005
0.5	0.2			1.009623	-1.994494	-0.270335	0.326925
	0.5			1.032564	-2.018926	-0.267405	0.322924
	0.8			1.055400	-2.043248	-0.264552	0.319032
	1			1.070566	-2.059402	-0.262691	0.316496
	0.2	1		0.788889	-1.815409	-0.586469	0.713419
		1.5		0.512257	-1.592897	-0.964381	1.180524
		2		0.157111	-1.309534	-1.428607	1.760578
		0.5	1	1.232959	-2.128344	-0.270335	0.326925
			2.0	0.664424	-1.831947	-0.270335	0.326925
			3.0	-1.013464	-2.223032	-0.270335	0.326925
			5.0	-2.850275	4.443846	-0.270335	0.326925

2) An increase in M increases fluid as well as particle phase velocities.
3) An increment in M decelerates fluid velocity, but particle velocity inclines in left part of the channel and declines in the right part of the channel.
4) With an increase in Cross flow Reynolds number the fluid velocity decreases near the left boundary and increases near the right boundary. Similar behavior is noted in the case of particle temperature. As R increases a decline in fluid temperature is observed.
5) With an increase in R, skin friction and Nu increase on both walls. With an increase in M the reverse behavior is observed on both walls. With an increase in β_t, γ, L skin friction and Nu increases on the left wall and decreases on the right wall.

Nomenclature

r, θ Polar coordinates,

α Angle of the channel,

υ Kinematic viscosity ($m^2 s^{-1}$),

μ Coefficient of viscosity ($kgm^{-1}s^{-1}$)

ρ Density of the fluid $\left(\frac{kg}{m^3}\right)$,

u Fluid phase velocity (ms^{-1})

u_p Particle phase velocity (ms^{-1}),

S Drag coefficient of the interaction for the force exerted by one face on the other

T Fluid phase temperature (K)

T_p Particle phase temperature (K)

U_0 Radial velocity along center line (LT^{-1}).

V_0 Suction/ Injection velocity at $r = r_0$ (LT^{-1})

β^* Coefficient of thermal expansion

σ Electric conductivity of the fluid (Sm^{-1})

H_0 Magnetic field intensity

μ_e Magnetic permeability of the fluid

ρ_P Density of the particle (Kgm^{-3})

C_P Specific heat of the fluid (JKg^{-1} K)

C_m Specific heat of the particles (JKg^{-1} K)

Q_0 Heat generation coefficient, (wm^{-3})

K Thermal conductivity of the fluid ($wm^{-1}k^{-1}$)

Re Reynolds number $\left(\frac{U_0 r_0}{\upsilon}\right)$

R Cross flow Reynolds number $\left(\frac{V_0 r_0}{\upsilon}\right)$

L Ratio of the densities of the particle and fluid phase $\left(\frac{\rho_p}{\rho}\right)$

β Fluid particle interaction parameter for velocity $\left(\frac{sr^2}{\upsilon}\right)$

M^2 Magnetic parameter $\left(\frac{\sigma H_0^{\,2} \mu_e^{\,2} r^2}{\rho \upsilon}\right)$

Gr Grashof number $\left(\frac{g\beta^* T_w r^3}{\upsilon^2}\right)$

Pr Prandtl number $\left(\frac{\mu c_p}{k}\right)$

Q Heat source parameter $\left(\frac{Q_0}{\rho c_p \upsilon}\right)$

γ Specific heat ratio $\left(\frac{c_m}{c_p}\right)$

References

Alam, S., & Khan. M. (2014). MHD diverging effects on mixed convection flow through a diverging channel with circular obstacle. *Proceedia Engineering, 90*, 403-410. doi:10.1016/j.proeng.2014.11.869

Banks, W., Drazin, P., & Zaturska. M. (1988). On perturbation of Jeffery-Hamel flow. *Journal of Fluid Mechanics, 186*, 559-581. doi:10.1017/S0022112088000278

Baris, S. (2003). Flow of a second grade visco-elastic fluid in aporous converging channel. *Turkish Journal of Engineering Environmental Science, 27*, 73-81.

Barzegar, G., Rahimi Takami, M., & Ganji. D. (2015). Investigation of thermal radiation on traditional Jeffery–Hamel flow to stretchable convergent/divergent channels. *Case Studies in Thermal Engineering, 6*, 28–39. doi:10.1016/j.csite.2015.04.002

Chamkha, A. (1995). Hydromagnetic two-phase flow in a channel. *International Journal of Engineering Science, 33*, 437-446. doi:10.1016/0020-7225(93)E0006-Q

Chamkha, A., & Al-Rashidi, S. (2010). Analytical solutions for hydromagnetic natural convection flow of a particulate suspension through isoflux-isothermal channels in the presence of a heat source or sink. *Energy Conversion and Management, 51*, 851-858. doi:10.1016/j.enconman.2009.11.021

Eldesoky, I., Abdelsalam, S., Abumandour, R., Kamel, M., & Vafai, K. (2017). Interaction between compressibility and particulate suspension on peristaltically driven flow in planar channel. *Applied Mathematics and Mechanics, 38*(1), 137-154. doi:10.1007/s10483-017-2156-6

Fakour, M., Vahabzadeh, A., Ganji, D. D., & Hatami, M. (2015). Analytical study of micropolar fluid flow and heat transfer in a channel with permeable walls. *Journal of Molecular Liquids, 204*, 198-204. doi:10.1016/j.molliq.2015.01.040

Ghaedamini, H., Lee, P., & Teo, C. (2013). Developing forced convection in converging diverging microchannels. *International Journal of Heat and Mass Transfer, 65*, 491–499. doi:10.1016/j.ijheatmasstransfer.2013.06

Ghadikolaei, S., Hosseinzadeh, K., & Ganji, D. (2018). MHD radiative boundary layer analysis of micropolar dusty fluid with graphene oxide (Go) engine oil nano particles in a porous medium over a streching sheet with Joule heating effect. *Powder Technology, 338*, 425-437. doi:10.1016/j.powtec.2018.07.045

Ghadikolaei, S. S., Hosseinzadeh, K., Yassari, M., Sadeghi, H., & Ganji, D. D. (2018). Analytical and numerical solution of non-Newtonian second grade fluid flow on a streching sheet. *Thermal Science and Engineering Process, 5*, 309-316. doi:10.1016/j.tsep.2017.12.010

Gholinia, M., Gholinia, S., Hosseinzadeh, K., & Ganji, D. (2018). Investigation on ethylene gltcol Nano fluid flow over a verticle permeable circular cylinder under effect of magnetic field. *Results in Physiscs, 9*, 1525-1533. doi:10.1016/j.rinp.2018.04.070

Hatami, M., Sheikholeslami, M., Hosseini, M., & Ganji, D. D. (2014). Analytical investigation of MHD nanofluid flow in non-parallel walls. *Journal of Molecular liquids, 194*, 251-259. doi:10.1016/j.molliq.2014.03.002

Hatami, M., Sheikholeslami, M., & Ganji, D. (2014). Nano fluid flow and heat transfer in an asymmetric porous channel with expanding and contracting wall. *Journal of Molecular liquids, 195*, 230-239. doi:10.1016/j.molliq.2014.02.024

Hatami, M., Hosseinzadeh, K., Domairry, G., & Behnamfar, M. T. (2014). Numerical study of MHD two-phase Couette flow analysis for fluid-particle suspension between moving parallel plates. *Journal of the Taiwanian Institute of Chemical Engineers, 45*(5), 2238-2245. doi:10.1016/j.jtice.2014.05.018

Jeffery, G. B. (1915**).** The two dimensional steady motion of a viscous fluid. *Philosophical Magazine Series 6, 29*, 455-465. doi:10.1080/14786440408635327

Krupalakshmi, K., Gireesha, B., Gorla, S., & Mahanthesh, B. (2016). Effects of diffusion –thermo and thermo diffusion on two-phase boundary layer flow past a stretching sheet with fluid –particle suspension and chemical reaction: A numerical study. *Journal of the Nigerian Mathematical Society, 35*, 66-81. doi:10.1016/j.jnnms.2015.10.003

Mallikarjuna, B., Rashad, A., Chamkha, A., & Hariprasad Raju, S. (2016). Chemical reaction effects on MHD convective heat and mass transfer flow past a rotating vertical cone embedded in a variable porosity regime. *Afrika Mathematika, 27*(3), 645-665. doi:10.1007/s13370-015-0372-1

Mallikarjuna, B., Rashad, A., Hussein, A., & Hariprasad Raju, S. (2016). Transportation and thermophoresis effects on non-Darcy convective flow over a rotating cone with thermal radiation. *Arabian Journal for Science and Engineering, 41*, 4691-4700. doi:10.1007/s13369-016-2252-x

Mansour, A., & Chamkha, A. (2003). Analytical solutions for hydromagnetic natural convection flow of a particulate suspension through a channel with heat generation or absorption effects. *Heat and Mass Transfer, 39*, 701-707. doi:10.1007/s00231-002-0355-2

Mir, A., Umar, K., Naveed, A., Raheela, M., & Syed, T. (2013). MHD flow of a Jeffery fluid in converging and diverging channels. *International Journal of Modern Mathematical Sciences, 6*(2), 92-106.

Mohammadreza, A., & Rouzbe, R. (2016). MHD copper-water nanofluid flow and heat transfer through convergent-divergent channel. *Journal of Mechanical Science and Technology, 30*(10), 4679-4686. doi:10.1007/s12206-016-0938-3

Mohammad, K., Islam, E., Prilal, M., & Ramzan, A. (2015**).** Slip effects on peristaltic transport of a particle-fluid suspension in a planar channel. *Applied Bionics and Biomechanics, Article ID 703574*. doi:10.1155/2015/703574

Mustafa, T. (2014). Extending the traditional Jeffery-Hamel flow to stretchable convergent/divergent channels. *Computers and Fluids, 100*, 196–203. doi:10.1016/j.compfluid.2014.05.016

Ramprasad, S., Subba Bhatta, S., Mallikarjuna, B., & Srinivasacharya, D. (2017). Two-phase particulate suspension flow in convergent and divergent channels: A Numerical Model. *International Journal of Applied and Computational Mathematics, 3*, 843-858. doi:10.1007/s40819-017-0386-5

Ramprasad, S., Subba Bhatta, S., & Mallikarjuna, B. (2018). Slip effects on MHD convective Two-phase particulate suspension flow in a divergent channel. *Defects and Diffusion forum, 388*, 303-316. doi:10.4028/www.scientific.net/DDF.388.303

Rawat, S., Bhargava, R., Kapoor, S., Beg, O., Beg, T., & Bansal, R. (2014). Numerical modeling of two-phase hydromagnetic flow and heat transfer in a particle-suspension through a non-Darcian porous channel. *Journal of Applied Fluid Mechanics, 7*(2), 249-261.

Rita, C., & Kamal, D. (2011). Hydromagnetic divergent channel flow of a visco elastic electrically conducting fluid. *International Journal of Engineering Science and Technology, 3*(10), 7556-7561.

Sadia, S., Naheed, B., & Anwar, M. (2017). Compressible dusty gas along a vertical wavy surface. *Applied Mathematics and Computation, 293*, 600-610. doi:10.1016/j.amc.2016.08.037

Sahoo, R., & Sastri, V. (1997). Numerical investigation of free convective flow in divergent channels. *Computer Methods in Applied Mechanics and Engineering, 146*, 31-41. doi:10.1016/S0045-7825(96)01228-5

Shadloo, M. S., & Kimiaeifar, A. (2010). Application of homotopy perturbation method to find an analytical solution for magnetohydrodynamic flows of visco-elastic fluids in converging/diverging channels. *Proceedings of the Institute of Mechanical Engineers Part C Journal of Mechanical Engineering Science 225*(2), 347- 353. doi:10.1243/09544062JMES2334

Sinharoy, J., & Nayak, P. (1982). Steady two dimensional incompressible laminar visco-elastic flow in a converging and diverging channel. *Acta Mechanica, 43*, 129-136. doi:10.1007/BF01175821

Sivakumar, C., Sreenath, K., & Pushpavanam, S. (2010). Experimental and numerical investigations of two-Phase (liquid-liquid) flow behavior in rectangular microchannels. *Industrial and Engineering Chemistry Research, 49*, 893–899. doi:10.1021/ie900555e

Terril, R. M. (1965). Slow laminar flow in a converging or diverging channel with suction at one wall and blowing at the other wall. *Journal of Applied Mathematics and Physics*, 16(2), 306-308. doi:10.1007/BF01587656

Umar, K., Naveed, A., & Syed, T. M. (2015). Soret and Dufour effects on flow in converging and diverging channels with chemical reaction. *Aerospace and Technology, 49*, 135-143. doi:10.1016/j.ast.2015.12.009

Usha, R., Senthilkumar, S., & Tulapurkara, E. (2006). Numerical study of particulate suspension flow through wavy-walled channels. *International Journal for Numerical Methods in Fluids, 51*(3), 235-259. doi:10.1002/fld.1115

Verma, P., Aruna, K., & Jeevan, S. M. (1998). Magnetic fluid flow in a two dimensional diverging channel. *International Journal of Engineering Science, 36*(7), 913-919. doi:10.1016/S0020-7225(97)00113-4

Yilmaz, O., Akyatan, A., & Senocak, E. (1998). Slow flow of the Reiner-Rivlin fluid in a converging or diverging channel with Suction and Injection. *Turkish Journal of Engineering and Environmental Sciences, 22*(3), 179-183.